Published in final edited form as:
J Biomech. 2011 August 11; 44(12): 2201–2206. doi:10.1016/j.jbiomech.2011.06.011.

Role of the Acetabular Labrum in Load Support Across the Hip Joint

Corinne R. Henak[1], **Benjamin J. Ellis**[1], **Michael D. Harris**[1], **Andrew E. Anderson**[1,2], **Christopher L. Peters**[2], and **Jeffrey A. Weiss**[1,2]

[1]Department of Bioengineering, and Scientific Computing and Imaging Institute, University of Utah, 72 S. Central Campus Drive, Salt Lake City, UT 84112

[2]Department of Orthopaedics, University of Utah, 30 North 1900 East, Rm. 3B165, Salt Lake City, UT 84132

Abstract

The relatively high incidence of labral tears among patients presenting with hip pain suggests that the acetabular labrum is often subjected to injurious loading *in vivo*. However, it is unclear whether the labrum participates in load transfer across the joint during activities of daily living. This study examined the role of the acetabular labrum in load transfer for hips with normal acetabular geometry and acetabular dysplasia using subject-specific finite element analysis. Models were generated from volumetric CT data and analyzed with and without the labrum during activities of daily living. The labrum in the dysplastic model supported 4-11% of the total load transferred across the joint, while the labrum in the normal model supported only 1-2% of the total load. Despite the increased load transferred to the acetabular cartilage in simulations without the labrum, there were minimal differences in cartilage contact stresses. This was because the load supported by the cartilage correlated to the cartilage contact area. A higher percentage of load was transferred to the labrum in the dysplastic model because the femoral head achieved equilibrium near the lateral edge of the acetabulum. The results of this study suggest that the labrum plays a larger role in load transfer and joint stability in hips with acetabular dysplasia than in hips with normal acetabular geometry.

Keywords

acetabular labrum; hip; cartilage mechanics; finite element; dysplasia

1. Introduction

The labrum is a fibrocartilagenous ring surrounding the acetabulum in the hip. It is triangular in cross-section, approximately 4.7 mm wide at the bony attachment by approximately 5.5 mm tall (Seldes et al., 2001). The labrum is primarily composed of

Corresponding Author: Jeffrey A. Weiss, PhD, Department of Bioengineering, University of Utah, 72 South Central Campus Dr., Room 3750, Salt Lake City, UT 84112, Phone: 801-587-7833, FAX: 801-585-5361, jeff.weiss@utah.edu.

Conflict of Interest Statement: The authors do not have any financial and personal relationships with other people or organisations that could inappropriately influence (bias) the work.

circumferential Type I collagen fibers (Petersen et al., 2003). The extent of the labrum medial to the acetabular rim varies by subject and location in the acetabulum (Seldes et al., 2001; Won et al., 2003).

Labral tears are often diagnosed in a clinical setting, suggesting that the labrum can be subjected to substantial loads in vivo (Blankenbaker et al., 2007; Burnett et al., 2006; Fitzgerald, 1995; Guevara et al., 2006; Leunig et al., 2004; Leunig et al., 1997; McCarthy and Lee, 2002; McCarthy et al., 2001; Neumann et al., 2007; Seldes et al., 2001; Wenger et al., 2004). There is an increased incidence of labral tears, labral hypertrophy, and labral calcification in hips that exhibit acetabular dysplasia (Dorrell and Catterall, 1986; Groh and Herrera, 2009; Guevara et al., 2006; Haene et al., 2007; Klaue et al., 1991; Leunig et al., 2004; Leunig et al., 1997), which suggests that the geometry of the dysplastic hip results in increased loads on the labrum in comparison to the normal hip.

Several studies have investigated the function of the labrum, but have not clearly determined the mechanical role of the labrum in the normal and dysplastic hip (Adeeb et al., 2004; Ferguson et al., 2000; Ferguson et al., 2000; Ferguson, 2001; Hlavacek, 2002; Konrath et al., 1998; Miozzari et al., 2004). In a cadaveric study of normal hips, removal of the labrum had no effect on contact stresses on the acetabular cartilage (Konrath et al., 1998). However, only the mid-stance of walking was simulated and the magnitude of the loads that were used in the study were about half of previously measured values for walking (Bergmann et al., 2001). Other studies reported that the labrum acts as a fluid seal on the joint during slow loading over longer periods of time (Adeeb et al., 2004; Ferguson et al., 2000; Ferguson et al., 2000; Ferguson et al., 2003; Hlavacek, 2002). It remains unclear whether the labrum contributes to joint stability and load transfer across the hip joint during activities of daily living.

The contribution of a structure to the mechanical function of a joint can be characterized by the percent of load supported by the structure across the joint. The aim of this study was to determine the load supported by the labrum and the cartilage contact stresses for a representative normal hip and a representative hip with acetabular dysplasia using subject-specific finite element modeling. Parametric studies examined how assumptions regarding the location of the boundary between acetabular cartilage and labrum and the assumed constitutive model for the labrum affected model predictions.

2. Methods

Two human subjects were selected from a series of 6 patients with traditional acetabular dysplasia and 18 normal volunteers that were recruited as part of a separate study. All subjects gave informed consent and were included following IRB approval. Patients with symptomatic acetabular dysplasia were screened with anteroposterior (A-P) radiographs. Those with lateral center-edge angles less than 20° were identified as having traditional acetabular dysplasia. Normal volunteers had no history of hip pathology or pain.

A subject with representative acetabular geometry was selected from each population. The patient (female, 35 years old, 66 kg) had a 17° center-edge angle and 19° acetabular index, which approximately matched the median values for the patient population. The shallow acetabulum and lateral under-coverage seen in dysplastic patients are characterized by center-edge angles below 25° and acetabular indices above 10° (Clohisy et al., 2008). Similarly, a normal subject (male, 30 years old, 87 kg) was selected that approximately matched the median center-edge angle and acetabular index of the population of normal volunteers (32° center-edge angle, 9° acetabular index).

Volumetric image data were acquired using CT arthrography (Figure 1). Approximately 20 ml of a 2:1 mixture of 1% lidocaine hydrochloride to Iohexol (Omnipaque 350, GE Healthcare, Princeton, NJ) was injected into the joint space. CT images were acquired with a field of view encompassing the entire pelvis and both femurs (342 mm for the dysplastic patient, and 331 mm for the normal volunteer), 512×512 acquisition matrix, and 1 mm slice thickness. Subjects were imaged under traction to increase the joint space and thus improve contrast between the acetabular and femoral cartilage (Anderson et al., 2008).

Segmentation of volumetric CT data was performed with a combination of thresholding and manual techniques, using the Amira software (Visage Imaging, Inc., San Diego, CA). Because the resolution of the segmentation mask was tied to voxel size, images were resampled to a higher resolution prior to segmentation (1536×1536 matrix, 0.23×0.23×0.33 mm^3 effective voxel size in the dysplastic patient and 0.22×0.22×0.33 mm^3 effective voxel size in the normal subject). The boundary between the cartilage and labrum was not visible in CT image data, so the initial boundary was defined where the concave acetabulum transitioned into the convex acetabular rim (Figure 2). A previous investigation demonstrated that the extent of the labrum on the medial side of the acetabular rim is variable (Won et al., 2003). Therefore, a second boundary was placed approximately 2 mm medial to the baseline boundary to assess the effects of the labrum extending medial to the acetabular rim (Figure 2).

Element formulations and mesh densities for bones and cartilage were based on our previous study (Anderson et al., 2008) (Figure 3). Cortical bone was represented with shell elements (Hughes and Liu, 1981), with a position-dependent thickness (Anderson et al., 2005). Cartilage and labrum were represented with hexahedral elements (Puso, 2000; Simo and Taylor, 1991). Hexahedral meshes for the cartilage and labrum were generated from the segmented surfaces using TrueGrid (XYZ Scientific, Livermore, CA). All meshes were generated directly from the segmented surfaces, with no assumptions regarding the geometry of the articular surfaces. A mesh convergence study was performed for the labrum.

Constitutive models for bone and cartilage were identical to those in our previous study (Anderson et al., 2008). Cortical bone was represented as isotropic linear elastic (E = 17 GPa, ν = 0.29) (Dalstra and Huiskes, 1995). Cartilage was represented as neo-Hookean hyperelastic (G = 13.6 MPa, K = 1359 MPa) (Park et al., 2004). The labrum was represented as transversely isotropic hyperelastic (Quapp and Weiss, 1998). The matrix strain energy was chosen to yield the neo-Hookean constitutive model with shear modulus C_1. The equations describing the material behavior of the fibers included material coefficients that scaled the exponential stress (C_3), specified the rate of collagen uncrimping (C_4), specified the modulus of straightened collagen fibers (C_5), and specified the stretch at which the collagen was straightened (λ^*).

Labrum material coefficients were determined by fitting the constitutive equation to an experimentally-derived expression for uniaxial stress-strain behavior along the fiber direction (C_1 = 1.4 MPa, C_3 = 0.05 MPa, C_4 = 36, C_5 = 66 MPa, λ^* = 1.103) (Ferguson, 2001). Material incompressibility was assumed when determining material coefficients because labrum is less permeable than cartilage (Athanasiou et al., 1995; Ferguson, 2001; Mow et al., 1980) and cartilage has been demonstrated to behave as an incompressible elastic material over the loading frequencies in activities of daily living (Ateshian et al., 2007). To yield nearly incompressible material behavior, the bulk modulus was specified to be 3 orders of magnitude greater than C_1 The primary fiber direction was oriented circumferentially (Petersen et al., 2003).

Boundary conditions were chosen to simulate heel strike during walking (WHS, 233% body weight), mid-stance during walking (WMS, 203% body weight), heel strike while ascending stairs (AHS, 252% body weight) and heel strike while descending stairs (DHS, 261% body weight). Neutral pelvic and femoral orientation was established using anatomical landmarks (Bergmann et al., 2001). The orientation of the applied load and the femur relative to the pelvis were based on instrumented implant and gait data (Bergmann et al., 2001). The magnitude of applied load was scaled by subject body weight (Bergmann et al., 2001). The pubis and sacro-iliac joints were fixed rigidly in space (Anderson et al., 2008). Motion was applied superiorly to the distal femur. The femur was allowed to move in the medial-lateral and anterior-posterior directions to achieve equilibrium in the acetabulum. Four springs (k = 1 MPa) were used at the distal femur to remove rigid-body modes from the simulation. Tied and sliding contact algorithms based on the mortar method were used (Puso, 2004; Puso and Laursen, 2004). One sliding interface was defined between the femoral and acetabular cartilage, while a second interface was defined between the femoral cartilage and labrum. Models were analyzed with and without the labrum. Frictionless contact was assumed for all contact interfaces. The friction coefficient between articulating cartilage surfaces is very low, on the order of 0.01-0.02 in the presence of synovial fluid (Caligaris and Ateshian, 2008; Charnley, 1960; Schmidt and Sah, 2007). Therefore, it is reasonable to neglect frictional shear stresses between contacting articular surfaces. Models were preprocessed using PreView (http://mrl.sci.utah.edu/software.php), analyzed using the nonlinear implicit solver NIKE3D (Puso, 2007), and postprocessed using PostView (http://mrl.sci.utah.edu/software.php).

Parameter studies were completed to assess the effects of modeling assumptions. To assess the effect of material assumptions, a neo-Hookean constitutive model matched to that used for the simulated cartilage was substituted for the transversely isotropic constitutive model. Additionally, the labrum fiber stiffness was changed ±50% in the transversely isotropic constitutive model. To examine the effect of anatomical angles, the anatomical adduction angle was changed ±3° (approximately 1 standard deviation (Bergmann et al., 2001)) in all loading scenarios. Finally, the applied load was changed ±30% (approximately one standard deviation (Bergmann et al., 2001)) in WHS in the dysplastic model.

Percent load supported by the labrum, average contact stress on the articular cartilage, contact area on the articular cartilage, and deflection of the labrum were determined. Percent load was calculated from the ratio of contact interface force to applied load. Cartilage contact stress was sampled on the surface of the acetabular cartilage. Cartilage contact area was calculated by summing the surface area of each element in the acetabular cartilage that was in contact with the femoral cartilage. Total deflection of the labrum was sampled through the thickness and maximum values were obtained.

3. Results

The labrum in the normal model supported 1-2% of the applied load, and the labrum in the dysplastic model supported 4-11% (Figure 4). The femoral head in the normal model achieved equilibrium in the center of the acetabulum, while the femoral head in the dysplastic model achieved equilibrium near the lateral edge of the acetabulum (Figure 5). When the cartilage-labrum boundary was moved medially, the percent load on the labrum increased 2- to 9-fold (Figure 6).

Changing the constitutive model from transversely isotropic to isotropic increased the load supported by the labrum 2-11% (Figure 7) and decreased the maximum deflection of the labrum 0-0.1 mm. The maximum deflection of the labrum occurred primarily in the radial direction and in approximately the same posterior-superior portion of the labrum for all

loading scenarios (Figure 5C, asterisk). In the transversely isotropic labrum, the maximum deflection was 1.3 mm in WHS and WMS, and 1.5 mm in AHS and DHS. The maximum deflection of the labrum was 0.1 mm smaller in the isotropic labrum in WHS, WMS and AHS, but did not change in DHS.

Cartilage contact areas demonstrated small increases in most simulations without the labrum and correlated to the load supported by the cartilage (Figure 8), while average and peak cartilage contact stresses demonstrated minimal changes. Average cartilage contact stress in the normal model with the labrum was 1.1, 0.9, 1.3, and 1.0 MPa in WHS, WMS, AHS, and DHS, respectively. Average cartilage contact stress in the normal model without the labrum was 1.1, 0.9, 1.2, and 1.0 MPa in WHS, WMS, AHS, and DHS, respectively. Average cartilage contact stress in the dysplastic model with the labrum was 0.8, 0.8, 0.5, and 1.2 MPa in WHS, WMS, AHS, and DHS, respectively. Average cartilage contact stress in the dysplastic model without the labrum was 0.8, 0.8, and 1.1 MPa in WHS, WMS, and DHS, respectively. When the dysplastic model was used to simulate AHS without the labrum, the femoral head dislocated from the acetabulum, precluding calculation of average pressures. Peak cartilage contact stresses were between 6 MPa and 14 MPa for all simulations.

Altering fiber stiffness ±50% in the transversely isotropic constitutive model only changed the labrum load support 0-1%. Changes of ±3° in anatomical adduction angle only changed labrum load support 0-1%. Changing the applied force ±30% did not alter labrum load support.

4. Discussion

The purpose of this study was to examine the role of the acetabular labrum in load transfer for hips with normal acetabular geometry and acetabular dysplasia. The load supported by the labrum of the dysplastic hip was substantially larger than that of the normal hip for all simulated activities. This was due to the shallow acetabulum in the dysplastic model, which caused the femoral head to achieve equilibrium near the lateral edge of the acetabulum. Since the dysplastic model exhibited lateral under-coverage, scenarios with loading vectors that were oriented more laterally (e.g., WMS) caused the labrum to support the highest loads. In contrast, the femoral head in the normal model achieved equilibrium near the center of the acetabulum, resulting in relatively low loads on the labrum.

Cartilage contact stresses were only slightly altered when the labrum was removed, despite the increased force on the acetabular cartilage. Contact area on the articular cartilage correlated to the load supported by the cartilage, therefore there were minimal changes in stress with and without the labrum (Figure 8). This is consistent with the results of a previous experimental study, which reported that removal of the labrum had no significant effect on cartilage contact stresses in cadaveric hips (Konrath et al., 1998). Taken together, these results suggest that the labrum functions to stabilize the joint, rather than to decrease cartilage contact stresses, during activities of daily living.

Average contact stresses on the acetabular cartilage were slightly lower than those reported in previous studies (Anderson et al., 2008; Brown and Shaw, 1983; Konrath et al., 1998). However, average stresses must be compared with caution because a threshold is often used when reporting experimental measurements of contact stress, based on the minimum stress that can be detected (e.g., pressure-sensitive film ranges, 2.4 MPa and 1.7 MPa (Anderson et al., 2008; Konrath et al., 1998)). When results for average contact stress in this study were recalculated with thresholds matching experimental studies, the average stresses were in better agreement with the results of the studies referenced above. Peak contact stresses compared well to results from previous *in vitro* studies (Adams and Swanson, 1985; Afoke

et al., 1987; Anderson et al., 2008; Brown and Shaw, 1983; von Eisenhart et al., 1999) and computational studies that used non-idealized geometry (Anderson et al., 2008; Brown and DiGioia, 1984).

The labrum supported more load when it was represented with an isotropic constitutive model than when it was represented with a transversely isotropic constitutive model. This result may seem counterintuitive at first glance, since the fiber stiffness (C_5) in the transversely isotropic constitutive model was larger than the shear modulus (C_1) in the isotropic constitutive model. Therefore, the transversely isotropic labrum could be expected to support greater loads and exhibit less deflection. However, the fibers were rarely loaded in tension during the simulations. Thus, the shear modulus (C_1) governed the material response of the labrum in simulations using both constitutive models. This also explains why changes to the fiber stiffness had a minimal effect. Many fiber-reinforced soft tissues are subjected to in situ stress (e.g., (Gardiner and Weiss, 2003)), which results in a stiffer material response for a given applied load. If in situ stresses were considered in these simulations, the fibers would support more load, thus yielding the expected result of increased load support with the addition of fiber reinforcement. However, given the current limitations in the literature, the constitutive model derived from bovine labrum data is expected to yield the most accurate model predictions.

Assumptions regarding the multiaxial material behavior of the labrum were necessary in this study because previous characterization of the material behavior of the labrum only performed material testing along the fiber direction. Two studies have reported material properties of human labrum. One tested pathologic tissue (Ishiko et al., 2005), and one reported only linear tensile and compressive moduli (Smith et al., 2009). The most complete characterization was performed using bovine labrum (Ferguson, 2001). From these data, the toe region along the fiber direction was assumed to represent the matrix response in all directions since multiaxial testing was not performed. In addition to uncertainty about the material behavior of the normal labrum, labra in dysplastic hips may have altered material properties due to effects such as hypertrophy and calcification (Klaue et al., 1991; Leunig et al., 2004; Leunig et al., 1997).

Parameter studies quantified the sensitivity of the simulations to assumed inputs. Large changes in load supported by the labrum with different boundaries between labrum and cartilage indicate that this boundary should be considered carefully in future modeling studies. This is particularly true when the models are generated from image data, in which the boundary is not visible. While these differences highlight the impact of this parameter on model results, the parameter study was not intended to address the possible clinical consequences of the boundary between cartilage and labrum. Changes in the magnitude of joint reaction force had no effect on the percent load supported by the labrum. Thus, the absolute load supported by the labrum scaled linearly with the joint reaction force, and the differences in kinematics between activities dictated any differences in percent load supported by the labrum. Since changes to adduction angle had minimal effect on percent load supported by the labrum, the direction of the applied load was more important than the anatomical orientation of the joint. This result is further demonstrated when comparing WHS and WMS. In WMS, the adduction angle of the load vector is larger than for WHS, and the labrum in the dysplastic model supported more load. This result is consistent with the findings of previous studies, which reported that the orientation of the abductor force affected predictions of stress in the acetabular cartilage, especially in simulations with small center-edge angles (Armand et al., 2005; Genda et al., 2001).

This study did not examine the possible effects of the sealing role of the labrum on predicted cartilage stresses and load support. Previous modeling and experimental studies suggest that

the sealing role of the labrum may influence various aspects of hip biomechanics (Adeeb et al., 2004; Ferguson et al., 2000; Ferguson et al., 2000; Ferguson et al., 2003; Hlavacek, 2002). However, there is no direct evidence in the literature that the sealing role of the labrum influences loadsharing between the articular cartilage and labrum or contract pressure distributions during activities of daily living. The differences in loading conditions and frequency in the previous studies make it difficult to predict how the results could be interpreted in light of the present study. Activities of daily living such as walking primarily involve compressive forces across the joint, with a frequency of about 1 second (Bergmann et al., 2001). Based on the permeability of the labrum and articular cartilage, there should be minimal fluid exudation from these tissues during a cyclic loading over 1 second (Ateshian et al., 2007; Ferguson, 2001). While it may be possible to extend the present model to assess the influence of a labral seal, this was beyond the scope of the present study.

The normal subject and patient that were analyzed in this study were chosen because their acetabular geometries were representative of the means of their parent populations. Due to variance of geometry in the parent populations, it is possible that selection of different subjects from the parent populations would lead to different conclusions. Nevertheless, the results of this study strongly suggest that the labrum plays a larger role in load transfer and joint stability in hips with acetabular dysplasia than in hips with normal acetabular geometry.

Acknowledgments

Financial support from NIH #R01AR053344 and #R01GM083925 is gratefully acknowledged.

References

Adams D, Swanson SA. Direct measurement of local pressures in the cadaveric human hip joint during simulated level walking. Annals Of The Rheumatic Diseases. 1985; 44:658–666. [PubMed: 4051586]

Adeeb SM, Sayed Ahmed EY, Matyas J, Hart DA, Frank CB, Shrive NG. Congruency effects on load bearing in diarthrodial joints. Computer Methods In Biomechanics And Biomedical Engineering. 2004; 7:147–157. [PubMed: 15512758]

Afoke NY, Byers PD, Hutton WC. Contact pressures in the human hip joint. The Journal Of Bone And Joint Surgery. 1987; British Volume 69:536–541. [PubMed: 3611154]

Anderson AE, Ellis BJ, Maas SA, Peters CL, Weiss JA. Validation of finite element predictions of cartilage contact pressure in the human hip joint. Journal Of Biomechanical Engineering. 2008; 130:051008–051008. [PubMed: 19045515]

Anderson AE, Ellis BJ, Peters CL, Weiss JA. Cartilage thickness: factors influencing multidetector CT measurements in a phantom study. Radiology. 2008; 246:133–141. [PubMed: 18096534]

Anderson AE, Peters CL, Tuttle BD, Weiss JA. Subject-specific finite element model of the pelvis: development, validation and sensitivity studies. Journal Of Biomechanical Engineering. 2005; 127:364–373. [PubMed: 16060343]

Armand M, Lepisto J, Tallroth K, Elias J, Chao E. Outcome of periacetabular osteotomy: joint contact pressure calculation using standing AP radiographs, 12 patients followed for average 2 years. Acta Orthopaedica. 2005; 76:303–313. [PubMed: 16156455]

Ateshian GA, Ellis BJ, Weiss JA. Equivalence between short-time biphasic and incompressible elastic material responses. Journal Of Biomechanical Engineering. 2007; 129:405–412. [PubMed: 17536908]

Athanasiou KA, Agarwal A, Muffoletto A, Dzida FJ, Constantinides G, Clem M. Biomechanical properties of hip cartilage in experimental animal models. Clinical Orthopaedics And Related Research. 1995:254–266. [PubMed: 7634715]

Bergmann G, Deuretzbacher G, Heller M, Graichen F, Rohlmann A, et al. Hip contact forces and gait patterns from routine activities. Journal Of Biomechanics. 2001; 34:859–871. [PubMed: 11410170]

Blankenbaker DG, De Smet AA, Keene JS, Fine JP. Classification and localization of acetabular labral tears. Skeletal Radiology. 2007; 36:391–397. [PubMed: 17226059]

Brown TD, DiGioia AM 3rd. A contact-coupled finite element analysis of the natural adult hip. Journal Of Biomechanics. 1984; 17:437–448. [PubMed: 6480619]

Brown TD, Shaw DT. In vitro contact stress distributions in the natural human hip. Journal Of Biomechanics. 1983; 16:373–384. [PubMed: 6619156]

Burnett RSJ, Della Rocca GJ, Prather H, Curry M, Maloney WJ, Clohisy JC. Clinical presentation of patients with tears of the acetabular labrum. The Journal Of Bone And Joint Surgery. 2006; American Volume 88:1448–1457. [PubMed: 16818969]

Caligaris M, Ateshian GA. Effects of sustained interstitial fluid pressurization under migrating contact area, and boundary lubrication by synovial fluid, on cartilage friction. Osteoarthritis And Cartilage / OARS, Osteoarthritis Research Society. 2008; 16:1220–1227.

Charnley J. The lubrication of animal joints in relation to surgical reconstruction by arthroplasty. Annals Of The Rheumatic Diseases. 1960; 19:10–19. [PubMed: 13809345]

Clohisy JC, Carlisle JC, Beaule PE, Kim YJ, Trousdale RT, et al. A systematic approach to the plain radiographic evaluation of the young adult hip. The Journal Of Bone And Joint Surgery. 2008; American Volume 90 4:47–66. [PubMed: 18984718]

Dalstra M, Huiskes R. Load transfer across the pelvic bone. Journal Of Biomechanics. 1995; 28:715–724. [PubMed: 7601870]

Dorrell JH, Catterall A. The torn acetabular labrum. The Journal Of Bone And Joint Surgery. 1986; British Volume 68:400–403. [PubMed: 3733805]

Ferguson SJ, Bryant JT, Ganz R, Ito K. The acetabular labrum seal: a poroelastic finite element model. Clinical Biomechanics (Bristol, Avon). 2000; 15:463–468.

Ferguson SJ, Bryant JT, Ganz R, Ito K. The influence of the acetabular labrum on hip joint cartilage consolidation: a poroelastic finite element model. Journal Of Biomechanics. 2000; 33:953–960. [PubMed: 10828325]

Ferguson SJ, Bryant JT, Ganz R, Ito K. An in vitro investigation of the acetabular labral seal in hip joint mechanics. Journal Of Biomechanics. 2003; 36:171–178. [PubMed: 12547354]

Ferguson SJ, Bryant JT, Ito K. The material properties of the bovine acetabular labrum. Journal of orthopaedic research. 2001; 19:887. [PubMed: 11562138]

Fitzgerald RH Jr. Acetabular labrum tears. Diagnosis and treatment. Clinical Orthopaedics And Related Research. 1995:60–68. [PubMed: 7634592]

Gardiner JC, Weiss JA. Subject-specific finite element analysis of the human medial collateral ligament during valgus knee loading. Journal Of Orthopaedic Research: Official Publication Of The Orthopaedic Research Society. 2003; 21:1098–1106. [PubMed: 14554224]

Genda E, Iwasaki N, Li G, MacWilliams BA, Barrance PJ, Chao EY. Normal hip joint contact pressure distribution in single-leg standing--effect of gender and anatomic parameters. Journal Of Biomechanics. 2001; 34:895–905. [PubMed: 11410173]

Groh MM, Herrera J. A comprehensive review of hip labral tears. Current Reviews In Musculoskeletal Medicine. 2009; 2:105–117. [PubMed: 19468871]

Guevara CJ, Pietrobon R, Carothers JT, Olson SA, Vail TP. Comprehensive morphologic evaluation of the hip in patients with symptomatic labral tear. Clinical Orthopaedics And Related Research. 2006; 453:277–285. [PubMed: 17016215]

Haene RA, Bradley M, Villar RN. Hip dysplasia and the torn acetabular labrum: an inexact relationship. The Journal Of Bone And Joint Surgery. 2007; British Volume 89:1289–1292. [PubMed: 17957065]

Hlavacek M. The influence of the acetabular labrum seal, intact articular superficial zone and synovial fluid thixotropy on squeeze-film lubrication of a spherical synovial joint. Journal Of Biomechanics. 2002; 35:1325–1335. [PubMed: 12231278]

Hughes TJR, Liu WK. Nonlinear finite element analysis of shells. I. Three-dimensional shells. Computer Methods in Applied Mechanics and Engineering. 1981; 26:331–62.

Ishiko T, Naito M, Moriyama S. Tensile properties of the human acetabular labrum-the first report. Journal Of Orthopaedic Research: Official Publication Of The Orthopaedic Research Society. 2005; 23:1448–1453. [PubMed: 16099616]

Klaue K, Durnin CW, Ganz R. The acetabular rim syndrome. A clinical presentation of dysplasia of the hip. The Journal Of Bone And Joint Surgery. 1991; British Volume 73:423–429. [PubMed: 1670443]

Konrath GA, Hamel AJ, Olson SA, Bay B, Sharkey NA. The role of the acetabular labrum and the transverse acetabular ligament in load transmission in the hip. The Journal Of Bone And Joint Surgery. 1998; American Volume 80:1781–1788. [PubMed: 9875936]

Leunig M, Podeszwa D, Beck M, Werlen S, Ganz R. Magnetic resonance arthrography of labral disorders in hips with dysplasia and impingement. Clinical Orthopaedics And Related Research. 2004:74–80. [PubMed: 15043096]

Leunig M, Werlen S, Ungersbock A, Ito K, Ganz R. Evaluation of the acetabular labrum by MR arthrography. The Journal Of Bone And Joint Surgery. 1997; British Volume 79:230–234. [PubMed: 9119848]

McCarthy JC, Lee JA. Acetabular dysplasia: a paradigm of arthroscopic examination of chondral injuries. Clinical Orthopaedics And Related Research. 2002:122–128. [PubMed: 12461363]

McCarthy JC, Noble PC, Schuck MR, Wright J, Lee J. The Otto E. Aufranc Award: The role of labral lesions to development of early degenerative hip disease. Clinical Orthopaedics And Related Research. 2001:25–37. [PubMed: 11764355]

Miozzari HH, Clark JM, Jacob HA, von Rechenberg B, Notzli HP. Effects of removal of the acetabular labrum in a sheep hip model. Osteoarthritis And Cartilage / OARS, Osteoarthritis Research Society. 2004; 12:419–430.

Mow VC, Kuei SC, Lai WM, Armstrong CG. Biphasic creep and stress relaxation of articular cartilage in compression? Theory and experiments. Journal Of Biomechanical Engineering. 1980; 102:73–84. [PubMed: 7382457]

Neumann G, Mendicuti AD, Zou KH, Minas T, Coblyn J, et al. Prevalence of labral tears and cartilage loss in patients with mechanical symptoms of the hip: evaluation using MR arthrography. Osteoarthritis And Cartilage / OARS, Osteoarthritis Research Society. 2007; 15:909–917.

Park S, Hung CT, Ateshian GA. Mechanical response of bovine articular cartilage under dynamic unconfined compression loading at physiological stress levels. Osteoarthritis And Cartilage / OARS, Osteoarthritis Research Society. 2004; 12:65–73.

Petersen W, Petersen F, Tillmann B. Structure and vascularization of the acetabular labrum with regard to the pathogenesis and healing of labral lesions. Archives Of Orthopaedic And Trauma Surgery. 2003; 123:283–288. [PubMed: 12802599]

Puso MA. A highly efficient enhanced assumed strain physically stabilized hexahedral element. International Journal for Numerical Methods in Engineering. 2000; 49:1029–64.

Puso MA. A 3D mortar method for solid mechanics. International Journal for Numerical Methods in Engineering. 2004; 59:315–336.

Puso MA, Laursen TA. A mortar segment-to-segment contact method for large deformation solid mechanics. Computer Methods in Applied Mechanics and Engineering. 2004; 193:601–629.

Puso, MA.; Maker, Bradley N.; Ferencz, Robert M.; Hallquist, John O. User's Manual. 2007. NIKE3D: A Nonlinear, Implicit, Three-Dimensional Finite Element Code For Solid and Structural Mechanics.

Quapp KM, Weiss JA. Material characterization of human medial collateral ligament. Journal Of Biomechanical Engineering. 1998; 120:757–763. [PubMed: 10412460]

Schmidt TA, Sah RL. Effect of synovial fluid on boundary lubrication of articular cartilage. Osteoarthritis And Cartilage / OARS, Osteoarthritis Research Society. 2007; 15:35–47.

Seldes RM, Tan V, Hunt J, Katz M, Winiarsky R, Fitzgerald RH Jr. Anatomy, histologic features, and vascularity of the adult acetabular labrum. Clinical Orthopaedics And Related Research. 2001:232–240. [PubMed: 11153993]

Simo JC, Taylor RL. Quasi-incompressible finite elasticity in principal stretches. continuum basis and numerical algorithms. Computer Methods in Applied Mechanics and Engineering. 1991; 85:273–310.

Smith CD, Masouros S, Hill AM, Amis AA, Bull AMJ. A biomechanical basis for tears of the human acetabular labrum. British Journal Of Sports Medicine. 2009; 43:574–578. [PubMed: 19042920]

Steppacher S, Tannast M, Werlen S, Siebenrock K. Femoral Morphology Differs Between Deficient and Excessive Acetabular Coverage. Clinical Orthopaedics and Related Research. 2008; 466:782–790. [PubMed: 18288550]

von Eisenhart R, Adam C, Steinlechner M, Muller-Gerbl M, Eckstein F. Quantitative determination of joint incongruity and pressure distribution during simulated gait and cartilage thickness in the human hip joint. Journal Of Orthopaedic Research: Official Publication Of The Orthopaedic Research Society. 1999; 17:532–539. [PubMed: 10459759]

Wenger DE, Kendell KR, Miner MR, Trousdale RT. Acetabular labral tears rarely occur in the absence of bony abnormalities. Clinical Orthopaedics And Related Research. 2004:145–150. [PubMed: 15346066]

Won YY, Chung IH, Chung NS, Song KH. Morphological study on the acetabular labrum. Yonsei Medical Journal. 2003; 44:855–862. [PubMed: 14584103]

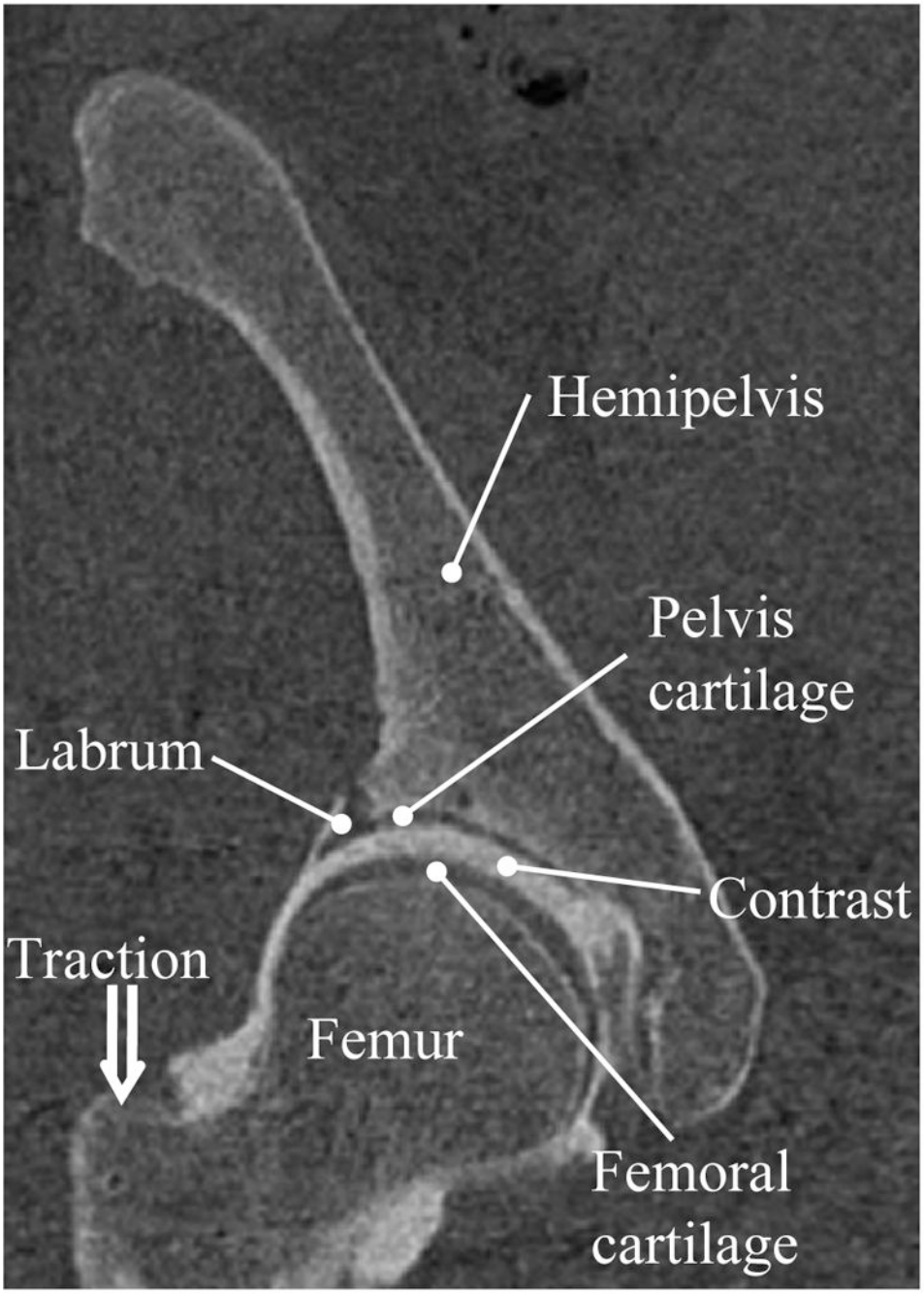

Figure 1.
Coronal CT slice of the dysplasia patient. Structures of interest are highlighted.

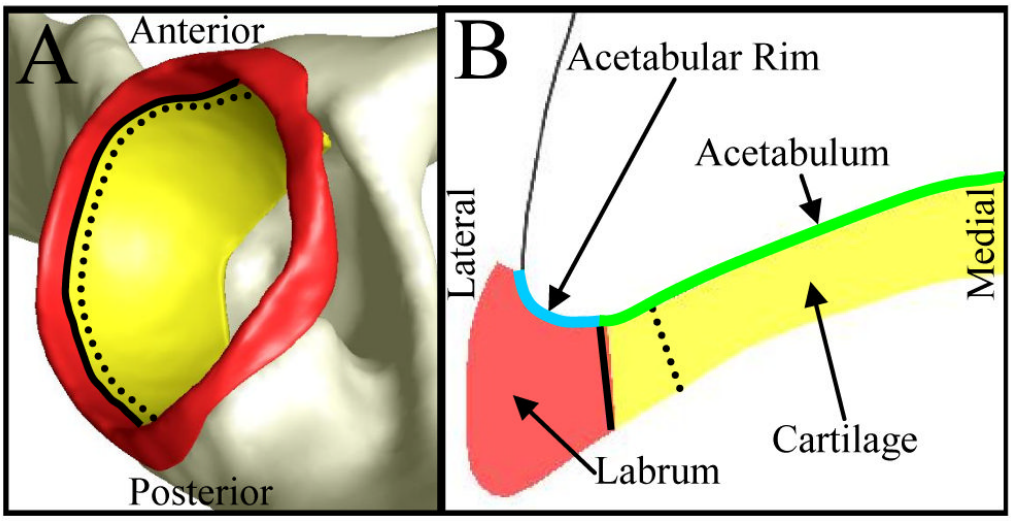

Figure 2.

Boundaries between the cartilage and labrum that were used in the model of the normal hip. The solid black line indicates the baseline boundary, while the dotted black line indicates the medial boundary, as described in the text. A – superior view, B – cross-sectional view through the superior portion of the acetabulum. The convex acetabular rim is outlined in cyan, and the concave acetabulum is outlined in green.

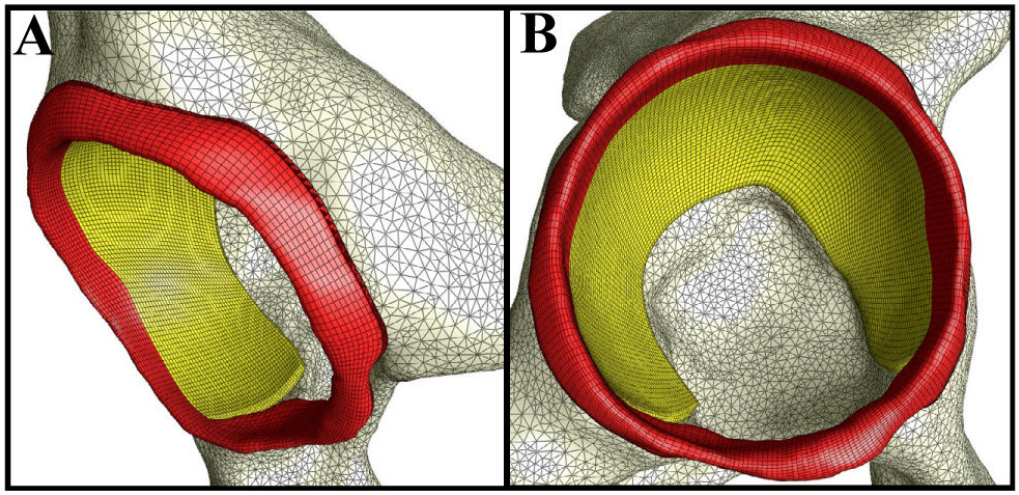

Figure 3.
Discretized hemipelvis (white), acetabular cartilage (yellow), and labrum (red) in the normal model. A – oblique view of shell and hexahedral meshes. B – medial view of shell and hexahedral meshes.

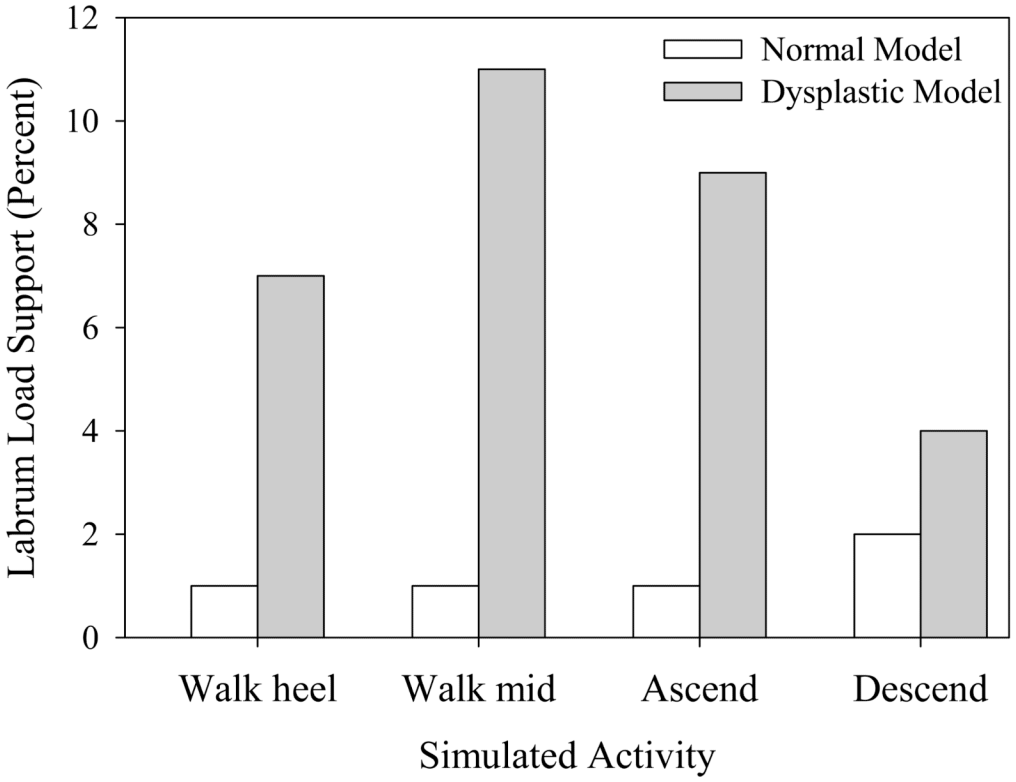

Figure 4.
Percent load on the labrum for the normal model and the dysplastic model. The labrum in the dysplastic model supported a higher percentage of load across the joint in all scenarios.

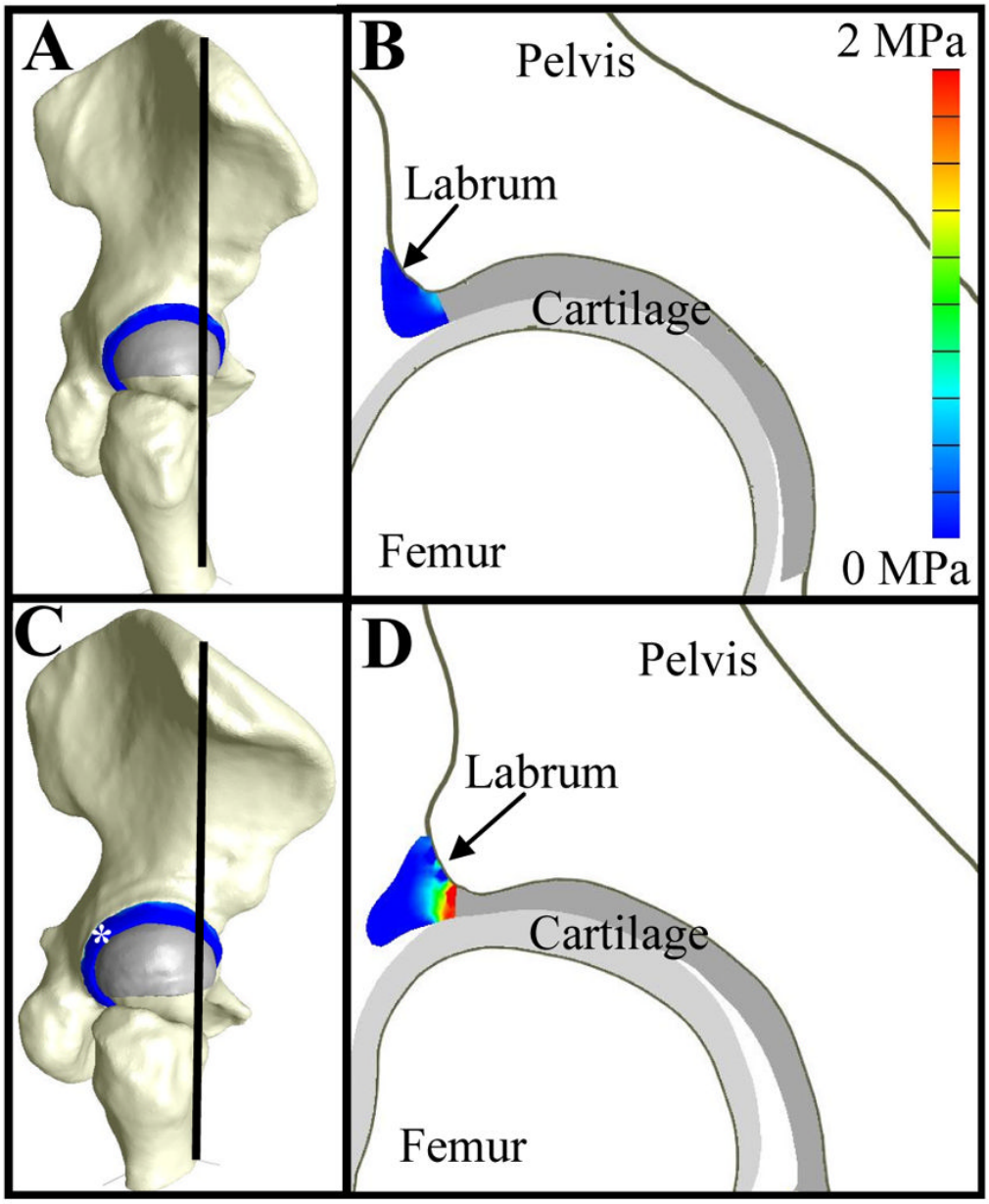

Figure 5.
Coronal cross-sectional views of contact stress on the anterosuperior labrum during walking heel strike. A – the black line indicates the slice location in the normal model. B – labrum contact stress in the normal model. C – the black line indicates the slice location in the dysplastic model. *The approximate location of maximum deflection in the labrum. D – labrum contact stress in the dysplastic model. The labrum in the dysplastic model was subjected to larger contact stress than the labrum in the normal model because the femoral head achieved equilibrium near the lateral acetabulum. Note the elliptical shape of the femoral head in the dysplastic model (Steppacher et al., 2008).

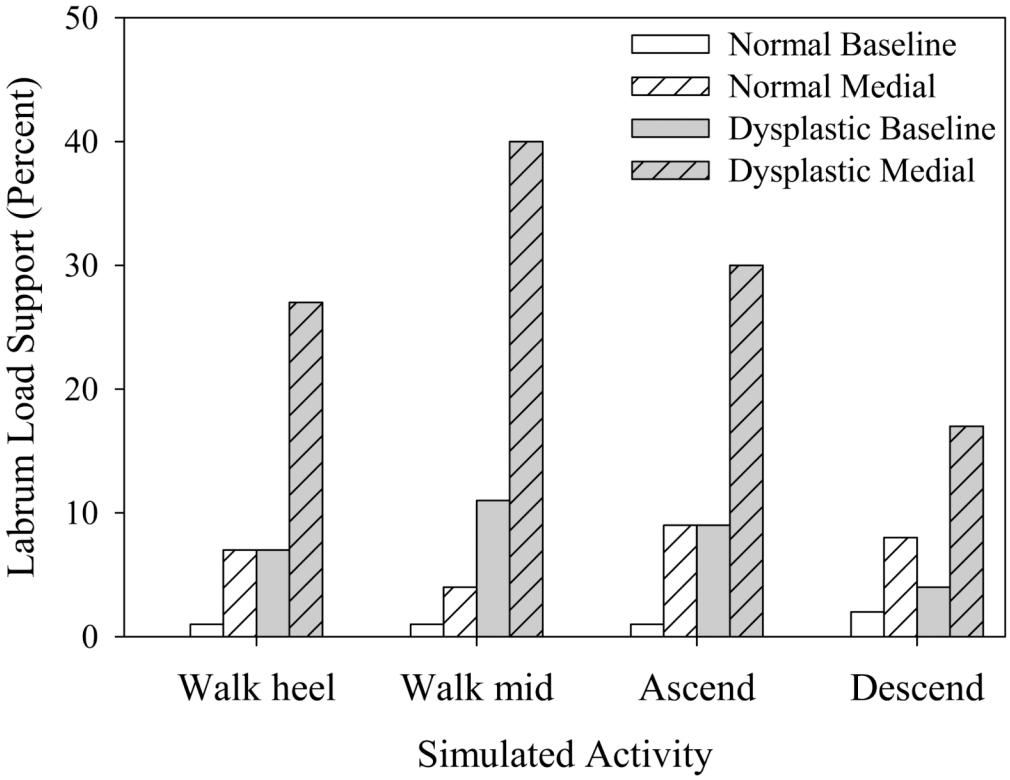

Figure 6.
Percent load supported by the labrum with baseline and medial cartilage-labrum boundaries. The medial boundary simulations demonstrated higher labrum load support for both subjects in all loading scenarios.

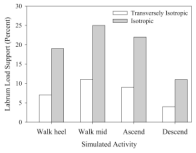

Figure 7.
Percent load supported by the labrum in the dysplastic model for 2 different constitutive models. The labrum supported more load when modeled with an isotopic constitutive model representative of cartilage.

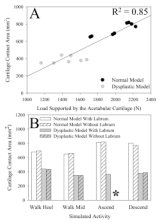

Figure 8.

Cartilage contact area. A – cartilage contact area correlated well with the force supported by the acetabular cartilage. B – cartilage contact area increased without the labrum in most loading scenarios. Cartilage contact area in the dysplastic model was lower than in the normal model. *When the dysplastic model was used to simulate AHS without the labrum, the femoral head dislocated from the acetabulum.